Development of Analytical Model of Bending Force during 3-Roller Conical Bending Process and Its Experimental Verification

Mahesh Chudasama, Harit Raval

Abstract—Conical sections and shells made from metal plates are widely used in various industrial applications. 3-roller conical bending process is preferably used to produce such conical sections and shells. Bending mechanics involved in the process is complex and little work is done in this area. In the present paper an analytical model is developed to predict bending force which will be acting during 3-roller conical bending process. To verify the developed model, conical bending experiments are performed. Analytical results and experimental results were compared. Force predicted by analytical model is in close proximity of the experimental results. The error in the prediction is ±10%. Hence the model gives quite satisfactory results. Present model is also compared with the previously published bending force prediction model and it is found that the present model gives better results. The developed model can be used to estimate the bending force during 3-roller bending process and can be useful to the designers for designing the 3-roller conical bending machine.

Keywords—Bending-force, Experimental-verification, Internal-moment, Roll-bending.

NOMENCLATURE

a = horizontal distance of the bottom roller centers in mm
E = Young's modulus in N/mm2
F, G, H = Anisotropy parameters
K = strength coefficient in N/mm2
M = bending moment in N-m
n = strain hardening exponent
P = Vertical load at the top roller and bending plate interface in N
$r1$ = radius of bottom roller in mm
R = radius of curvature of the bent plate in mm
t = thickness of the plate in mm
t_e = thickness of elastic layer in mm
U = Vertical distance travelled by the top roller for first stage of static bending in mm
w = width of the blank in mm
x = half the horizontal distance of the bottom roller centers in mm
y = distance of fiber from neutral plane in mm
y_{ep} = distance of the fiber upto which elasticity E is constant in mm
β = bottom roller inclination,
θ = Angle between frictional force and horizontal plane at the roller plate interface in radians
μ = coefficient of friction at roller plate interface
ε = strain
σ = stress in N/mm^2
$\bar{\varepsilon}$ = effective strain
$\bar{\sigma}$ = effective stress
ν = Poisson's ratio
χ = curvature of the bend plate between bottom rollers, mm^{-1}

Mahesh Chudasama is with Government Engineering College, Dahod, Gujarat (India) 389151 (Phone: +91 9979074377; e-mail-mkcgecs@gmail.com).
Harit Raval is with S.V. National Institute of Technology, Surat, Gujarat (India) 395007 (e-mail:hkraval1@yahoo.co.in).

I. INTRODUCTION

FOR erecting large towers for wind mills or for chimneys, conical sections or shells made up of thick metal plates are used. Apart from these such conical sections find other structural applications in the industries. These conical sections or shells are usually made by using roll bending process. Roll bending is one of the metal forming processes. Forming is the process of imparting the desired shape to the material by deforming the material beyond its elastic stress and below its fracture stress. The stresses induced in the forming operation are thus plastic stresses. Metal forming can be used to impart desired shape, size and finish to the material without significant loss of the material. Moreover, strength of the product is improved through improved stress flow lines. Continuous bending operation, in which a long strip of metal (typically coiled steel) is passed through consecutive sets of rollers or roller stands, until the desired cross sectional profile is obtained, is called roll bending.

The process of roll bending is used for many years for the production of the conical shells and sections. Still there is little research work available on the analysis of the process. The normal practice of plate roller bending still heavily depends upon the experience and the skill of the operator as well as designers. In industry, working to templates, or by trial and error, yet remains a common practice to be followed. In the present paper an attempt is made to give analysis of force requirement during the process.

The process of roll bending can be divided in four stages namely (i) static bending, (ii) Forward rolling, (iii) Backward rolling and (iv) unloading. Static bending is performed by loading the blank between top roller and bottom rollers as shown in Fig. 1 and then moving the top roller downwards. This process is similar to air bending process but is performed by the rollers instead of punch & die. In the next operation bottom rollers are given rotation initially in forward direction to perform the rolling. When the required length of the plate is bent the machine is stopped. In the next stage of the process the bottom rollers are driven in backward direction to complete the operation. In the final stage the top roller is pulled up and the rolled plate is unloaded.
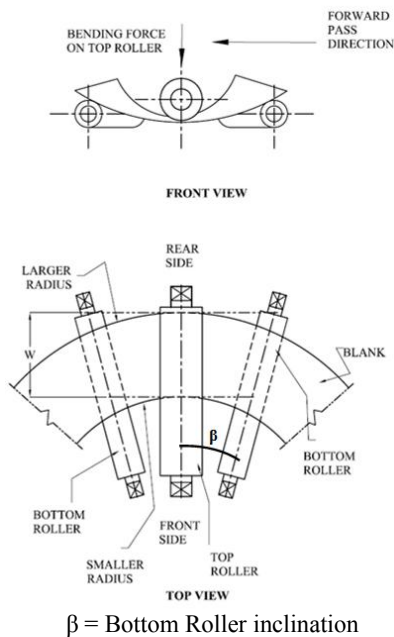
FRONT VIEW

REAR SIDE

β = Bottom Roller inclination

Fig. 1 Schematic arrangement of 3-roller conical bending setup

Analysis for bending is reported by many researchers. Mathematical models for plane-strain sheet bending have been established by Wang et al. to predict springback [1]. They used the true (non-linear) strain distribution across the sheet thickness. They concluded that the bending moment is greater for materials having higher strength, strain hardening and normal anisotropy. Hua has extensively worked over the analysis of 4-roller bending process. Hua et al. have proposed a mathematical model for determining the plate internal bending resistance at the top roll contact for multi-pass four-roll thin-plate bending operations [2].

For continuous single-pass four-roll thin plate bending an analytical model was proposed by Baines et. al., considering the equilibrium of the internal and external bending moment at and about the plate-top roll contact [3]. Hua and Lin had proposed a mathematical model to simulate the mechanics for four-roll thin plate bending process considering varying radius of curvature of the plate between the rollers [4]. Hua and Lin also analyzed for the four-roll plate bending process, the influence of material strain hardening on the mechanics of steady continuous roll and edge-bending [5]. Moreira and Ferron had investigated the influence of the plasticity model adopted in sheet metal forming simulations [6]. They showed that the isotropic hardening assumption gives a good fit of experiments for the tests where the sheet is submitted to relatively linear loading paths. Firat had studied rate-independent anisotropic plasticity models in the deformation modeling of a stamping part [7]. To predict spring back and bend allowance simultaneously in air bending Kim et al. have developed an analytical model and prepared computer program for the same [8].

Gandhi et al. had worked over the issue of machine setting parameters for required dimensions of the conical section

considering the springback for continuous multi-pass bending of cone frustum on 3-roller conical bending machines with non-compatible rollers [9], [10]. For cyclic bending under tension Sanchez presented an elastic–plastic mathematical model for plane strain flow of sheet metal subjected to strain rate effects [11]. He also included Bauschinger factors in the model for stress reversal. Chudasama and Raval had developed an approximate bending force prediction model for 3-roller conical bending model and discussed the effects of various parameters on the bending force [12].

Through the study of the available literature it can be conclude that most of the work reported by the researchers is for cylindrical bending processes. Preliminary investigation related to conical bending as far as bending force is concerned is done by A. H. Gandhi et al. [9], [10]. An attempt is made to address the problem of bending force prediction in this area by Chudasama & Raval [12], but it gives approximate estimation. So it is required to develop an analytical model which gives better estimation of the bending force for 3-roller conical bending process. Present work is for development of force prediction model for 3-roller conical bending process and experiments have been performed for the verification of model. The developed analytical model will be useful to the researchers to understand the complex mechanics of the process as well as the designers to optimize the designing process.

II. ANALYTICAL MODEL

Mechanics of cone frustum bending is complex to understand as compared to cylindrical shell bending. In 3-roller conical bending process first step is bending of the plate by lowering down the top roller. In this step it is required to exert force on the top roller to lower it, which will bend the plate. This vertical force exerted on the top roller will give the external bending moment required to bend the plate.

A. External Bending Moment

External bending moment over the plate exerted by the rollers can be derived by considering the geometry of the setup during bending. Hua et al. have insisted that it is difficult to have a single mathematical model that takes into account all the complexities of the bending process [2].The force pattern during conical bending is complicated and needs to be simplified. During bending there will be reaction forces on the bottom roller because of the top roller load. Indicative figure of the bottom roller with the reaction force is shown in Fig. 2. The weight of the plate, being less as compared to the forces that are acting on the plate during the bending, it is neglected. The rollers without the plate are shown for clarity of the explanation. In front view, cross section of the roller plate by vertical plane is shown and components along the vertical plane of the reaction forces over the roller are shown. Similarly in top view, the components of the reaction along the horizontal plane are shown in Fig. 2 (a). Bottom roller with different orientations along with the force is shown in Fig. 2 (b) to have more clarity over the complexity of the 3-dimensional force during the roll-bending process.
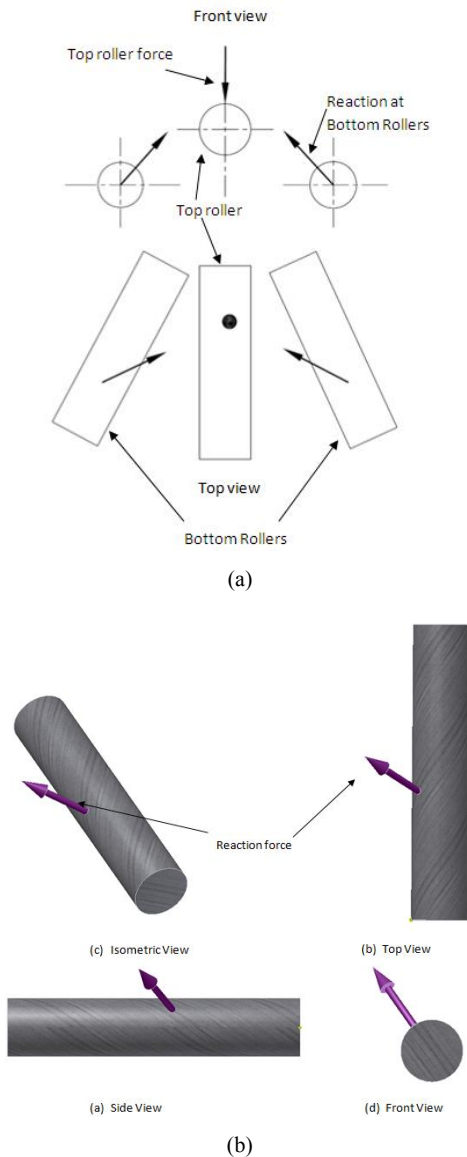
Front view

Top roller force

Reaction at
Bottom Rollers

Top roller

Top view

Bottom Rollers

(a)

Reaction force

(c) Isometric View

(b) Top View

(a) Side View

(d) Front View

(b)

Fig. 2 (a) Reactions at the bottom roller due to bending force on top roller, (b) Bottom roller with 3-dimensinal force pattern

It can be observed from the Fig. 2 that the reaction force at the bottom roller will have three components in mutually perpendicular directions. For the present case bottom rollers are rotated in horizontal plane. So the axial force for bottom roller will be the horizontal component of the reaction force and will be in horizontal plane.

In the derivation of external bending moment over the plate, forces in vertical plane passing through the three rollers and perpendicular to the top roller axis is considered. If axial forces on the bottom rollers are resolved, they will not have. Any component along the vertical plane, as bottom rollers are inclined only in horizontal plane as explained earlier. So axial force on the bottom rollers will not affect the derivation of the external bending moment derived earlier by Chudasama & Raval [12]. Reaction on the top roller will have three

components in mutually perpendicular directions. Axial force on the top roller will also not affect the external bending moment as it is not inclined in the vertical plane. In the present analysis vertical component of the force on top roller, 'P', is considered for the calculations.

Fig. 3 gives schematic of blank and roller arrangement for static bending. It is assumed here that the blank is having uniform/constant radius of curvature for the supported length of the blank between two bottom rollers. Equation for external bending moment can be derived as reported [12].

$$M_{total} = \frac{P}{2}\left(1 - \frac{x - r_1 \sin\theta}{a - r_1 \sin\theta}\right)\left(\frac{1}{\cos\theta + \mu\sin\theta}\right)(x - tan\theta(r_1 - U) + \mu(x * tan\theta - r_1(sin\theta * tan\theta + cos\theta - 1) - U)) \ (1)$$
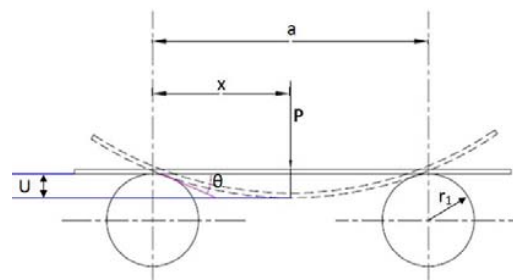

Fig. 3 Schematic of blank and roller arrangement for static bending

B. Internal Bending Moment

When top roller is lowered down to get the bending, the plate will resist the moment. Stresses will be developed in the plate and there will be internal bending moment in the plate opposing the external bending moment. Free body diagram of a plate element is shown in Fig. 4 (a). There will be 3-dimensional stress pattern as can be seen in Fig. 4 (a). Along with normal stresses there will be shear stresses acting over the plane. If we consider infinitesimal element of the plate and show the normal axis by x, y and the stress vector along the xy and xz can be shown by Fig. 4 (b).

Stresses
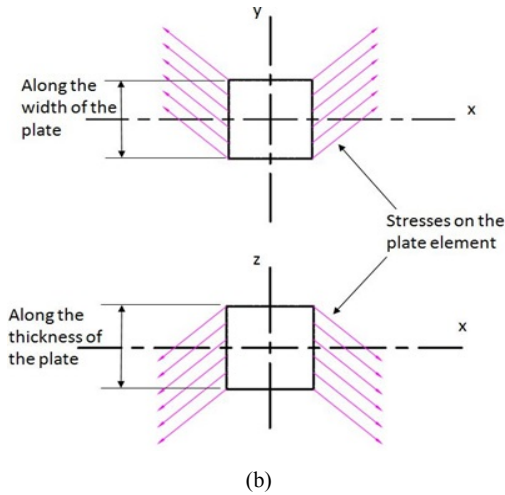
Plate element

(a)

(b)
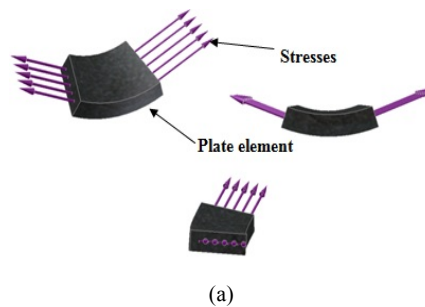
Fig. 4 Plate element with internal stresses (a) 3-Dimensional view (b) 2-Dimensional view

For the present analysis it is assumed that the principal stresses are lying along the normal axis, so shear stresses will be zero along the normal axis. Only the normal stresses will be considered for the analysis. So out of six components of stress tensor only three normal stress components will be considered in the formulation of the force equation.

To get the force equation it is required to have the relation of effective stress and effective strain with normal stresses and normal strains respectively. In the case considered here as the principal axis coincides with the symmetry axis, the shear stresses will be zero over the planes of the element.

For this condition as per theory proposed by Hill [13] and discussed by Hasek [14], effective stresses and strains can be related with corresponding normal stresses and strains by;

$$\bar{\sigma} = \left\{ \frac{3}{2} \frac{1}{F+G+H} \left[F(\sigma_y - \sigma_z)^2 + G(\sigma_z - \sigma_x)^2 + H(\sigma_x - \sigma_y)^2 \right] \right\}^{1/2} \quad (2)$$

$$d\bar{\varepsilon} = \left[\frac{2}{3}(F+G+H) \right]^{\frac{1}{2}} \left\{ \left[\frac{F(Gd\varepsilon_y - Hd\varepsilon_z)^2 + G(Fd\varepsilon_x - Hd\varepsilon_z)^2 + H(Fd\varepsilon_x - Gd\varepsilon_y)^2}{(FG+GH+HF)^2} \right] \right\}^{\frac{1}{2}} \quad (3)$$

In the present case it is assumed that width of the plate remains constant during the process. So the components σ_z, and ε_z will be zero. Also it is assumed that the thickness of the plate remains constant during the process. So the component ε_y will be zero. So for equivalent stress and equivalent strain relations for the 3-roller conical bending considering the biaxial deformation of a sheet having rotational symmetry (normal anisotropy & planar isotropy), (2) can be written as, [15]

$$\bar{\sigma} = \sqrt{ \frac{3}{2} \left[\left(\frac{1+r}{2+r} \right) \left\{ \sigma_x^2 + \sigma_y^2 - \left(\frac{2r}{1+r} \right) \sigma_x \sigma_y \right\} \right] } \quad (4)$$

& for the present case where there is no material loss, considering volume constancy, (3) can be written as, [15]

$$d\bar{\varepsilon} = \sqrt{ \frac{2}{3} \left[\frac{(2+r)(1+r)}{(1+2r)} \left\{ d\varepsilon_x^2 + d\varepsilon_y^2 + \left(\frac{2r}{1+r} \right) d\varepsilon_x d\varepsilon_y \right\} \right] } \quad (5)$$

where r is anisotropic index and for normal isotropy, i.e. r = Substituting r=1 in above (4) can be written as,

$$\bar{\sigma} = \sqrt{ \sigma_x^2 + \sigma_y^2 - \sigma_x \sigma_y } \quad (6)$$

For the effective strain, considering proportional loading $d\varepsilon_i$ is replaced by total strain ε_i [16] and by also putting r =1 in (5),

$$\bar{\varepsilon} = \sqrt{ \frac{2}{3} \left[2 \left\{ \varepsilon_x^2 + \varepsilon_y^2 + \varepsilon_x \varepsilon_y \right\} \right] } \quad (7)$$

For assuming $\frac{\sigma_y}{\sigma_x} = \alpha$ (constant), [17]

Putting the value of σ_x from above,

$$\bar{\sigma} = \left\{ \sigma_x^2 + \alpha^2 \sigma_x^2 - \alpha \sigma_x^2 \right\}^{\frac{1}{2}} \quad (8)$$

$$\bar{\sigma} = \sigma_x \left\{ 1 + \alpha^2 - \alpha \right\}^{\frac{1}{2}} \quad (9)$$

For the present case ε_y is zero, as thickness of the plate assumed constant in the process.

Putting $\varepsilon_y = 0$ in (7) above,

$$\bar{\varepsilon} = \sqrt{ \frac{2}{3} [2\{\varepsilon_x^2\}] }$$

$$\bar{\varepsilon} = \sqrt{ \frac{4}{3} } \varepsilon_x$$

$$\bar{\varepsilon} = \frac{2}{\sqrt{3}} \varepsilon_x \quad (10)$$

Now, as per power law, $\bar{\sigma} = K\bar{\varepsilon}^n$, putting the values of $\bar{\sigma}$ and $\bar{\varepsilon}$ from (9) and (10),

$$\sigma_x \{1 - \alpha + \alpha^2\}^{\frac{1}{2}} = K \left[\frac{2}{\sqrt{3}} \varepsilon_x \right]^n$$

$$\sigma_x = \frac{K \left[\frac{2}{\sqrt{3}} \right]^n}{\{1 - \alpha + \alpha^2\}^{\frac{1}{2}}} \varepsilon_x^n$$

$$\sigma_x = KD\varepsilon_x^n \quad (11)$$

where,

$$D = \frac{\left(\frac{2}{\sqrt{3}} \right)^n}{\{1 - \alpha + \alpha^2\}^{\frac{1}{2}}} \quad (12)$$

For elastic portion,

$$\bar{\sigma} = E\bar{\varepsilon}$$

$$\sigma_x \{1 - \alpha + \alpha^2\}^{\frac{1}{2}} = E \frac{2}{\sqrt{3}} \varepsilon_x \quad (13)$$

$$\sigma_x = E \frac{2}{\sqrt{3}} \left\{ \frac{1}{1 - \alpha + \alpha^2} \right\}^{\frac{1}{2}} \varepsilon_x \quad (14)$$

$$\sigma_x = EH\varepsilon_x \qu(15)$$

where,

$$H = \frac{2}{\sqrt{3}}\left\{\frac{1}{1-\alpha+\alpha^2}\right\}^{\frac{1}{2}} \tag{16}$$

Now, for the static bending of the plate the Power law material behavior is assumed in the plastic region. The bending moment can be split into an elastic contribution and plastic contribution and can be calculated from:

$$M_{total} = M_{elastic} + M_{plastic}$$
$$= 2\int_{elastic}\sigma_x y\, dy + \int_{plastic}\sigma_x y\, dy \tag{17}$$

To decide the limits of the integration, the neutral plane is assumed to be at the center line of the plate thickness. It is also assumed that the plate thickness 't' remains constant during the process.

Inserting the values of σ_x for elastic and plastic portion in (17), we get,

$$M_{total} = 2\int_0^{y_{ep}} E'H\varepsilon_x y\, dy + \int_{y_{ep}}^{t/2} KD\varepsilon_x^n y\, dy \tag{18}$$

For bending $\varepsilon_x = \frac{\sigma}{E} = \frac{y}{R}$, and E will be replaced by E', where $E' = \frac{E}{(1 - v^2)}$ [17], inserting the values in (18) for elastic portion,

$$M_{elastic} = 2\int_0^{y_{ep}} E'H\left(\frac{y}{R}\right)y\, dy \tag{19}$$

Assuming modulus of elasticity 'E' as constant,

$$M_{elastic} = 2H\left[\frac{E'}{R}\right]\left[\frac{y^3}{3}\right]_0^{y_{ep}} \tag{20}$$

$$= 2H\left[\frac{E'}{R}\right]y_{ep}^3 \tag{21}$$

$$M_{plastic} = 2\int_{y_{ep}}^{t/2} KD\varepsilon_x^n y\, dy \tag{22}$$

$$M_{plastic} = 2KD\int_{y_{ep}}^{t/2}\left(\frac{y}{R}\right)^n y\, dy \tag{23}$$

$$= 2KD\left(\frac{1}{R}\right)^n\left[\frac{y^{n+2}}{n+2}\right]_{y_{ep}}^{t/2} \tag{24}$$

$$= 2KD\left(\frac{1}{R}\right)^n\left[\frac{1}{n+2}\right]\left[\left(\frac{t}{2}\right)^{n+2} - y_{ep}^{n+2}\right] \tag{25}$$

$$M_{total} = 2H\left[\frac{E'}{R}\right]y_{ep}^3 + 2KD\left(\frac{1}{R}\right)^n\left[\frac{1}{n+2}\right]\left[\left(\frac{t}{2}\right)^{n+2} - y_{ep}^{n+2}\right] \tag{26}$$

Value of y_{ep} is determined by the relation proposed by Nepershin [18], and discussed by Chudasama & Raval [12] as,

$$y_{ep} = \frac{t_e}{2} = \frac{1}{E^*\chi} \tag{27}$$

C. Expression for Bending Load P

Equating (1) & (27), and rearranging,

$$M_{total} = 2H\left[\frac{E'}{R}\right]y_{ep}^3 + 2KD\left(\frac{1}{R}\right)^n\left[\frac{1}{n+2}\right]\left[\left(\frac{t}{2}\right)^{n+2} - y_{ep}^{n+2}\right] = \frac{P}{2}\left(1 - \frac{x-r_1\sin\theta}{a-r_1\sin\theta}\right)\left(\frac{1}{\cos\theta+\mu\sin\theta}\right)(x - \tan\theta(r_1 - U) + \mu(x*\tan\theta - r_1(\sin\theta*\tan\theta+\cos\theta-1) - U)) \tag{28}$$

$$P = \frac{\frac{4}{3}H\left[\frac{E'}{R}\right]y_{ep}^3 + 4KD\left(\frac{1}{R}\right)^n\left[\frac{1}{n+2}\right]\left[\left(\frac{t}{2}\right)^{n+2} - y_{ep}^{n+2}\right]}{\left(1 - \frac{x-r_1\sin\theta}{a-r_1\sin\theta}\right)\left(\frac{1}{\cos\theta+\mu\sin\theta}\right)(x - \tan\theta(r_1 - U) + \mu(x*\tan\theta - r_1(\sin\theta*\tan\theta+\cos\theta-1) - U))} \tag{29}$$

Equation (29) gives the bending force required to get the required bend. It can be observed that there are various parameters affecting the bending force. Material parameters like, strength coefficient 'K', strain hardening exponent 'n', yield stress 'σ_y'; Geometrical parameters like center distance between bottom rollers 'a', top roller position 'U', etc. In formulation bottom roller inclination β is not directly involved. But it explicitly affects the bending force. The relation for bottom roller inclination can be given as [9],

$$\beta = \tan^{-1}\left[\left(\frac{A_R - A_F}{2}\right)\left(\frac{1}{\cos\alpha}\right)\left(\frac{\sin^{\varphi}/2}{R_R - R_F}\right)\right] \tag{30}$$

where, β = bottom roller inclination,

AF, AR = Center distance between bottom rollers at front and rear end respectively

α = top roller inclination, in the present case it is zero

φ = Cone angle

RF, RR = Bending radius at the front end and rear end respectively

It can be observed that the value of bottom roller inclination for particular value of cone angle will affect the values of center distance of the roller bearings 'a' as well as the bend radius 'R', which in turn will affect the bending force

required. [12]. Equation (29) is similar to the bending force prediction model given earlier by Chudasama & Raval, [12], except that the present model contains constants 'H' and 'D'. These constants depend upon the stress ratio which affects the bending force requirements. Present model considers the effect of stress ratio on bending force, which was not there in previously stated model. To validate the developed analytical model experiments have been performed and the experimental setup and procedure is discussed in the subsequent section.

III. EXPERIMENTATION

A. Experimental Setup

Analytical model of force prediction developed in previous section is required to be validated through the experiments. 3-roller conical bending machine is used for the validation of the developed analytical model. CAD model for the same is shown in Fig. 5. The top roller and bottom rollers are supported on the spherical bearings. The bearings are placed in the recesses on the support frames using bearing blocks. The rollers can be inclined on their respective axis because of these spherical bearings placed at their ends. The bottom rollers of the machine are driven by two independently driven electric motors. When the bottom rollers are inclined there are

chances of misalignment of the roller bearing center and the motor shaft center. In such conditions to successfully transmit the torque to the rollers, they are attached with the motors using universal joints as shown in Fig. 6. The setup is also facilitated with the load cells at the top roller as well bottom roller bearings to measure the reaction in 3 mutually perpendicular planes as shown in Fig. 7. These load cells are attached to the online data acquisition system which gives the force reading during the continuous roll bending process.
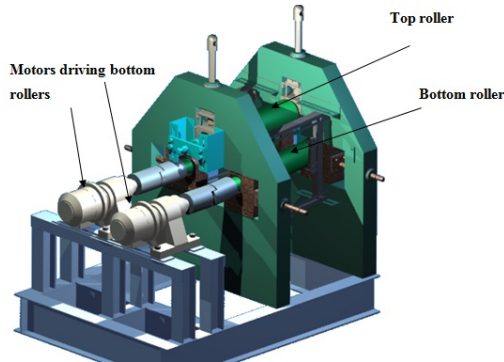
Fig. 5 CAD model of the experimental setup

Fig. 6 Bottom rollers driven by motors coupled by universal joints

Fig. 7 Load cells attached with the roller bearings

B. Material Selection

Structural steel FE 410 WA is widely used for the various structural applications and is easily available in Indian commercial market. Structural steel of material grade FE 410 WA as per IS 2062 (2006) is having material properties equivalent to C-Mn steel of material grade SA-516 G60 as per ASME sec II part A (2004). Hence, structural steel of material grade FE 410 WA as per IS 2062 (2006) is selected for cone frustum bending experiments.

Experimental runs at five different bottom roller

inclinations (β) and for five different blank thicknesses of 6, 8, 10, 12 and 14 mm to study the thickness effect on bending force requirements were planned. However, based on the availability of the blanks and measurement, the blank thicknesses used for the cone frustum bending experiments are observed to be 5.84, 7.87, 8.85, 11.84 and 13.97. Thickness of the blank is measured at 6 different places (3 each on reference and larger end blank edges) using the Vernier calliper. Average of these reading is taken as blank thickness.

To use the analytical model developed in the previous section it is required to find out the material properties like yield stress 'σ_y', strain hardening exponent 'n' and strength coefficient 'K'.Material properties are found as per the ASTM standards and reported as in Table I.

TABLE I
MATERIAL PROPERTIES DERIVED FROM TENSILE TESTING OF SPECIMENS

Plate Thickness (t) (mm)	Yield Stress (σ_y)	Strain Hardening Exponent(n)	Strength Coefficient (K) (N/mm^2)
5.84	600	0.1513	1031
7.87	278	0.2425	817
8.85	320	0.2502	897
11.84	346	0.2362	915
13.97	270	0.2427	913

Experiments have been performed by varying parameters affecting bending force requirements. Data of force required for the static as well dynamic roll bending have been acquired through the Data Acquisition System (DAS). Data has been processed and the sample result obtained for one of the thickness at different bottom roller inclination 'β' is shown in Table II. Plate before and after bending is shown in Fig. 8.
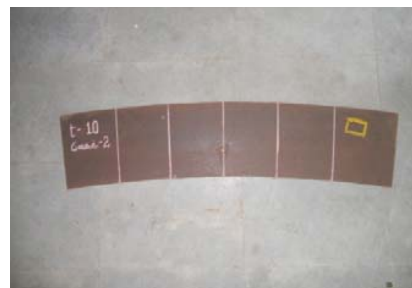
(a)

(b)

Fig. 8 (a) Plate before bending, (b) Plate after bending

Data obtained through the experimentation is to be used for the validation of the developed analytical model of force prediction. The validation is presented in subsequent section.

TABLE II
SAMPLE RESULT TABLE FOR T = 7.87 MM VARIATION OF B IN DEGREE

Plate Thickness (mm)	Plate Bend Radius At Larger End (mm)	Bottom Roller Inclination, β (Degree)	Top Roller Force (N)
7.87	696	0	885
7.87	780	0.93	912
7.87	869	1.86	899
7.87	963	2.79	655
7.87	1060	3.71	688

IV. VALIDATION OF MODEL FOR SINGLE PASS BENDING

As discussed in Section II, the bending force for single pass, 3-roller conical bending is calculated by (29). In the above equation value of constants 'H' and 'D' is calculated using the value of stress ratio 'σ_y/σ_x' available from literature [17]. Value of 'θ' is found out from the geometry of the bending using geometrical parameters. The value of yep can be found out using (27). Material properties were taken from Table I. Using the values of other process parameters like 'x', 'a', 'r1', etc involved in the above equation, analytical results for different thicknesses with variation of bottom roller inclination β are plotted as shown in Fig. 9 below. Experimental values measured during the experimentation are also plotted for different thicknesses as shown in Fig. 9.
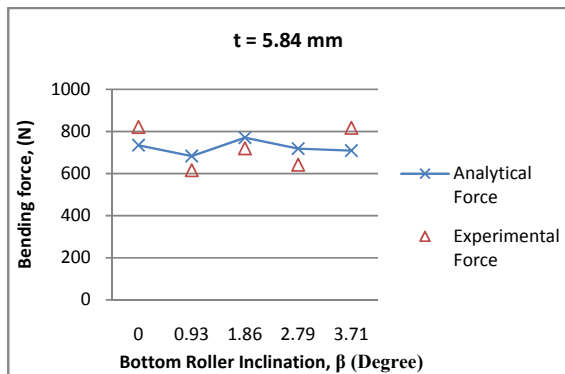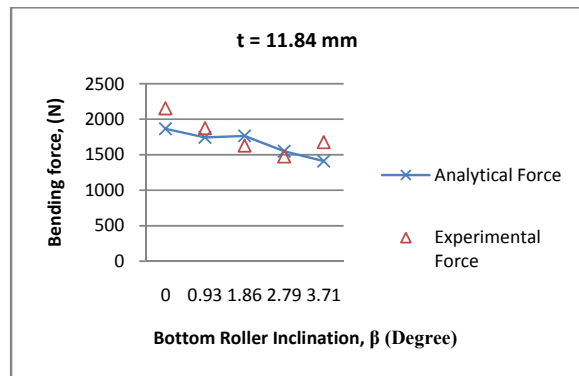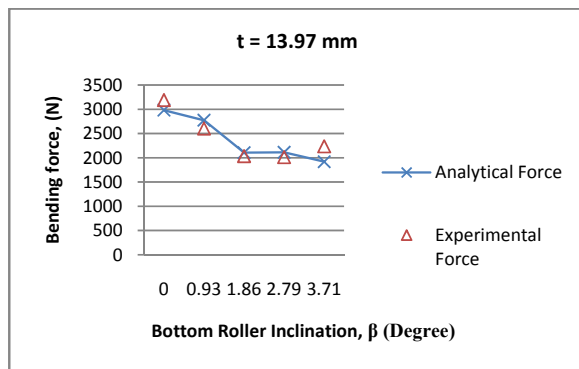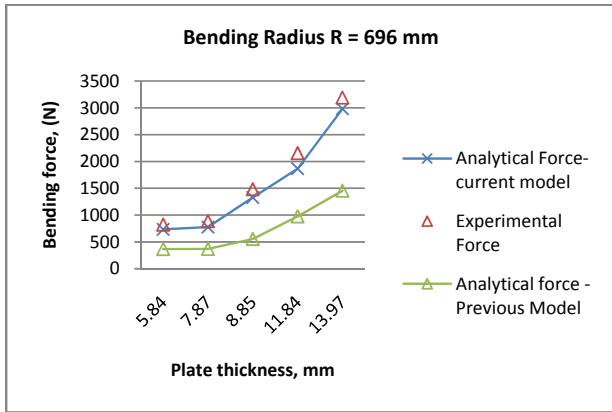
(a)
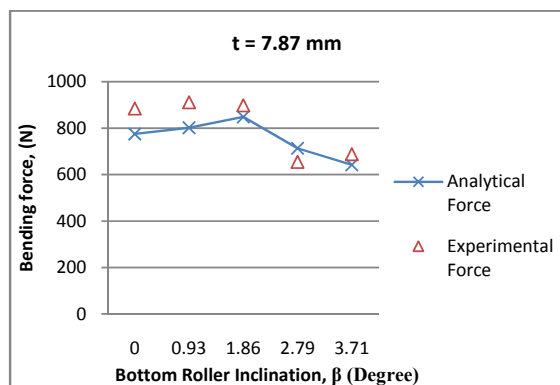
(b)
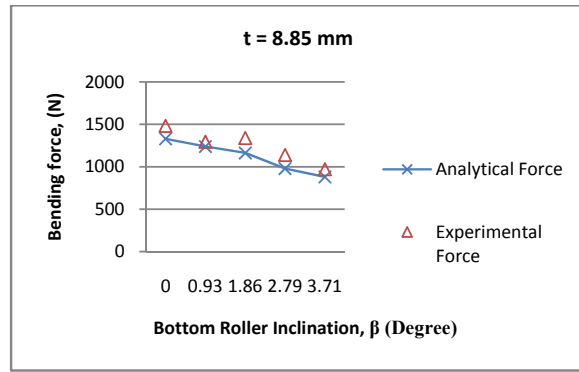
(c)

(d)

(e)

Fig. 9 Experimental and analytical bending force comparison for different thicknesses with respect to bottom roller inclination 'β', (a) thickness t = 5.84mm (b) thickness t = 7.87mm (c) thickness t = 8.85mm (d) thickness t = 11.84mm (e) thickness t = 13.97mm

It can be observed from Fig. 9 that as the bottom roller inclination 'β' increases the force required to bend the plate decreases. The predicted values of bending force by the analytical model are quite matching with the experimental values. Error observed in the force prediction is ±10%. The error can be because of various assumptions like isotropic material, principal axis coincide with the normal axis, etc. Considering the sensitivity of various measuring instruments individually as well as combined the error in analytical results

is in quite acceptable range. As the error in the predicted force with respect to experimental force required to bend the plate is in the acceptable range, the analytical model is validated and can be used for the force prediction in 3-roller conical bending with satisfactory accuracy.
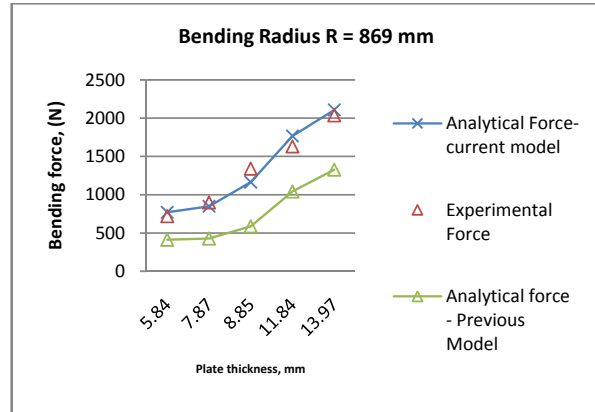
To compare the present analytical model with the approximate bending force prediction model given by Chudasama & Raval [12], comparison graphs of both analytical results with experimental results are plotted for different bend radius as shown in Fig. 10.
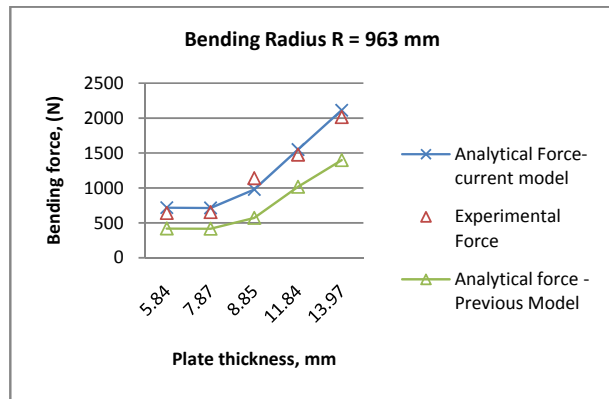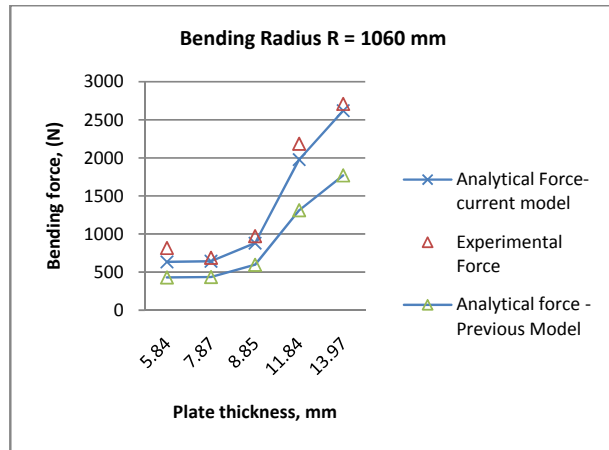
(a)
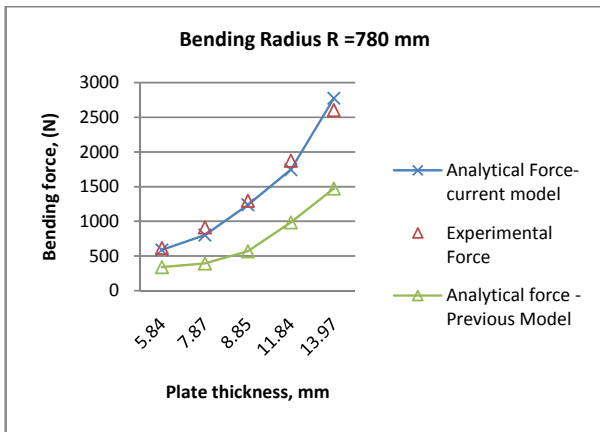
(b)

(c)

(d)

(e)

Fig. 10 Comparison of Experimental, current analytical model and Previous analytical model for different thicknesses with respect to bend radius, (a) Bend Radius R = 696mm, (b) Bend Radius R = 780mm, (c) Bend Radius, R = 869mm, (d) Bend Radius R = 963mm, (e) Bend Radius R = 1060mm

The bend radius is proportional to bottom roller inclination and as bend radius increases the bending force will increase [12]. The same is reflected by the experimental results also.

The present model not only follows this trend but also gives close proximity results with the experimental results as can be observed in Fig. 10. So the present model gives better estimation of the bending force required and can be used for the bending force prediction.

V. CONCLUSION

In the present paper analytical model is developed for prediction of the bending force in 3-roller conical bending process. External bending moment required to bend the plate has been equated to the internal bending resistance from the plate material to get the analytical expression of the bending force. Experiments have been performed for the validation of the obtained analytical model. Analytical results have been compared with the experimental results. It is found that analytical model for bending force prediction is in good accordance with the experimental results. Considering sensitivity of the measuring instruments the error is in the quite acceptable range and the model can be used for the force prediction during the 3-roller conical bending process. Present model is compared with the previously published approximate bending force prediction model [12]. It is found that the present model gives better accuracy than the previously published model. The present work carried out will give insight to the complex mechanics involved in 3-roller conical bending process to the researchers working in the area of metal forming. The model will also be useful to the designers associated with manufacturing firms of 3-roller conical bending machines.

ACKNOWLEDGMENT

REFERENCES

[1] Wang C., Kinzel G., Altan T., *Mathematical modeling of plane-strain bending of sheet and plate*, Journal of Materials Processing Technology, 1993, Vol-39, pp. 279–304.
[2] Hua M., Sansome D.H., Baines K., *Mathematical modeling of the internal bending moment at the top roll contact in multi-pass four-roll thin-plate bending*, Journal of Materials Processing Technology, 1995, Vol-52, pp. 425-459.
[3] Baines K., Hua M., Cole I.M., Rao K.P., *A formulation for determining the single-pass mechanics of the continuous four-roll thin plate bending process*, Journal of Materials Processing Technology, 1997, Vol- 67, pp. 189-194.
[4] Hua M., Lin Y.H., *Large deflection analysis of elastoplastic plate in steady continuous four-roll bending process*, International Journal of Mechanical Sciences, 1999, Vol-41, pp.1461-1483.
[5] Hua M., Lin Y.H., *Influence of strain hardening on continuous plate roll-bending process*, International Journal of Non-Linear Mechanics, 2000, Vol-35, pp. 883-896.
[6] Moreira L.P., Ferron G., *Influence of the plasticity model in sheet metal forming simulations*, Journal of Materials Processing Technology, 2004, Vol-155–156, 1596–1603.
[7] Firat M., *Computer aided analysis and design of sheet metal forming processes: Part II – Deformation response modeling*, Materials and Design, 2007, Vol-28, pp. 1304–1310.
[8] Kim H, Nargundkar N., Altan T., *Prediction of Bend Allowance and Springback in Air Bending*, ASME Transactions, 2007, 129, 342-351
[9] Gandhi A H, H. K. Raval, Analytical and Empirical Modeling of top roller position for 3-roller cylindrical bending of plates and its & experimental verification, Journal of Materials Processing Technology, 2008, 197, 268-278.
[10] Gandhi A. H., Shaikh A. A., Raval H. K., Formulation of springback and machine setting parameters for multi-pass three-roller cone frustum bending with change of flexural modulus, International Journal of Material Forming, 2009, 2, 45–57.
[11] Sanchez L. R, *A new cyclic anisotropic model for plane strain sheet metal forming*, International Journal of Mechanical Sciences, 2000, Vol-42, pp. 705-728.
[12] Chudasama M. K., Raval H. K., An approximate bending force prediction for 3-roller conical bending process, International Journal of Material Forming, 2013,Vol. 6 No 2 pp. 303-314.
[13] Hill R., The Mathematical theory of Plasticity, Oxford University Press, 1950.
[14] Hasek, V. V., "*An evaluation of the applicability of Theoretical Analyses to the Forming Limit Diagram*", Proc. Of 4th Int. Conf. On Fracture, 2, p. 476, June 1977.
[15] Wagoner R. H., Chenot J.L., Fundamentals of Metal forming, Willey eastern, 1997.
[16] Mielnik E., Metalworking Science and Engineering, McGraw Hill 1991.
[17] Marciniac Z., Duncan J.L., Hu S. J., Mechanics of sheet metal forming, Butterworth-Heinemann, 1992.
[18] Nepershin R. I., *Bending of a Thin Strip by a Circular Tool*, Mechanics of Solids, 2007, Vol-42-4, pp. 568-582.